GEOLOGICAL EVIDENCE FOR LATITUDE-DEPENDENT WATER-RELATED DEPOSITS ON MARS: IMPLICATIONS FOR CLIMATE HISTORY AND THE HYDROLOGICAL CYCLE ON MARS.

James W. Head, Department of Geological Sciences, Brown University, Providence, RI 02912 USA (james_head@brown.edu)

Part 1: Evidence for Non-Polar Ice Deposits: Introduction: Estimates of the total water abundance on Mars and the nature and magnitude of sources and sinks throughout its history has been a matter of controversy for decades [see summary in 1]; estimates range over several orders of magnitude. Because the nature of earliest Mars history and the processes operating then are so poorly known, our strategy has been to start with the present environment, when climate conditions are more well-known, and work backward in time, using the geologic record as a measure of the presence, location, and state of water. We first identify elements of the current water cycle, assess their volumes, and then turn to the Amazonian geological record to trace the history of the climate and water cycle as recorded in non-polar ice deposits. This inventory permits us to assess the migration paths and behavior of water during long-term climate change and to document changes in the nature and volumetric significance of the water cycle in the past geologic history of Mars. We first identify non-polar ice deposits and then assess their significance compared to the major surface reservoir on Mars, the current polar caps. Studies of the spin-axis/orbital parameter history of Mars provide a robust solution for climatic driving forces for the most recent ~20 Ma of martian history, but cannot be mapped further back into the past due to the chaotic nature of the solutions [2]. Recent Mars history is dominated by a global hyperarid very cold environment and glacial conditions at non-polar latitudes. Interpretations are assisted by an understanding of glacial and periglacial conditions in areas that are polar analogs to Mars (such as the Antarctic Dry Valleys) [3], and an understanding of the behavior of polar ice under different insolation conditions, using global climate models (GCMs) [4-5].

The Current Environment and Climate History: The current hydrological cycle on Mars is horizontally stratified, separated from the subsurface by a global permafrost layer [6]; seasonal variations and longer-term climate change result in migration between the largest reservoir (the polar caps), the atmosphere, vapor diffusion into and out of the regolith, and surface deposition in non-polar regions. Current polar layering is thought to be related to variations in spin-axis/orbital parameters [2]. These variations cause changes in insolation and climate, and corresponding variations in dust and volatile stability, mobility, transport and deposition [e.g., 7-8]. We outline examples of non-polar ice-related deposits that have implications for the climate history of Mars. **(1) The Latitude-Dependent Mantle and Recent Ice Ages:** Numerous lines of evidence show the presence of geologically very young, meters-thick, multiple latitude-dependent surface layers emplaced to 30° latitude in both hemispheres that were ice-rich when formed and whose deposition and modification were driven by spin-axis/orbital parameter induced climate change [summarized in 9]. Poleward of 60° the terrain is characterized by bumpy polygon-like features interpreted to be contraction-crack polygons, thought to mark the presence of shallow ice-rich deposits undergoing thermal cycling. A distinct pitted mantle texture between 30°-60° latitude is interpreted to be the dissected remnant of a former ice-rich dust deposit; associated viscous-flow features and gullies are seen in microenvironments in this zone [10]. These data compellingly point to climate-driven water ice and dust mobilization and emplacement during very recent periods of higher obliquity. Degradation and dissection of the deposit in mid-latitudes further point to recent climate change [11], perhaps reflecting return of mid-latitude ice to polar regions during the recent phase of lower obliquity [e.g., 7,9]. **(2) Northern High Latitude Cold-Based Glacial Crater Fill:** Lobate concentric ridges draped across crater walls/floors, and around central peaks have been interpreted to be drop moraines, deposited during the advance and retreat of a lobate cold-based glacier, originating on the crater rim [12]. **(3) Mid-High Latitude Concentric Crater Fill (CCF):** Initially thought to be ice-assisted talus creep [13], new data show details of morphology and structure that support the role debris-covered glaciers [14] related to regional glaciation [15]. **(4) Mid-Latitude Lineated Valley Fill (LVF) and Plateau Glaciation:** Interpreted earlier as vapor-diffusion-assisted emplacement of ice in slope-related talus causing plastic flow [13], new data strongly support some earlier interpretations [16] that debris-covered glacial flow formed regional valley glacial landsystems [17-18]. **(5) Mid-Latitude Lobate Debris Aprons (LDA):** Earlier thought to represent ice-assisted creep [13], the intimate association of LDA with LVF [19], and LDA internal structure and morphology now point to a debris-covered glacier mode of origin for many LDAs [20-21], recently confirmed by SHARAD data [22-23]. **(6) Mid-Latitude Ice Highstands:** Evidence of highstands of ice (e.g., perched lobes, trimlines, moraines) suggest that almost a kilometer of ice has been lost from LVF [24]. **(7) Low Mid-Latitude Phantom LDAs:** Evidence for the former presence of ice-rich deposits surrounding massifs at latitudes even lower than the LDA suggest former ice lobes [25] at even lower latitudes (<30°) than LDAs. **(8) Tropical Mountain Glaciers:** Fan-shaped deposits on the Tharsis Montes and Olympus Mons NW flanks represent huge tropical mountain glaciers [26-31] formed during periods of high obliquity [32] during the Late Amazonian. **(9) Near-Equatorial Outflow Channel Rim Deposits:** Glacial-like features on the Mangala Valles outflow channel (18°S) rim suggest that earlier Amazonian climate was cold enough near the equatorial to cause glaciation, rather than runoff [33]; lack of evidence of melting suggests that the water outflow did not radically change the climate. **(10) Pedestal and Excess-Ejecta Craters (EEC):** Recent analysis of pedestal craters has shown their latitudinal distribution [34] and revealed strong evidence for ice below pedestal protective veneers [35]. EEC characteristics [36-37] further support regional mid-high latitude ice cover during the Amazonian and thicknesses of several tens to over a hundred meters. Some adjacent areas show evidence for related ice-rich deposits of comparable thickness [38]. **(11) South Circumpolar Ice Cap: The Hesperian Dorsa Argentea Formation:** The set of Hesperian-aged south circumpolar deposits represented by the Dorsa Argentea Formation [DAF; 39-40] has

been interpreted to be a volatile-rich polar deposit [40] representing more than twice the area of the present Amazonian-aged layered terrain and residual polar ice, which it currently underlies. The deposit characteristics (e.g., smooth, pitted and etched deposits, pedestal craters, sinuous ridges interpreted as eskers, fluvial channels around the margins, and marginal plains thought to be remnants of ponds and lakes, etc.) have been interpreted to indicate that the DAF contained significant quantities of water ice, and that it represented an ancient circumpolar ice sheet [40].

Discussion and Conclusions: 1) Current Volatile Inventory: The current polar caps are the dominant active reservoir in the present water cycle; estimates of current volume and global equivalent layer (GEL) thickness are (North, 1.14 x 10^6 km^3, GEL ~7.8 m; South, 1.2 x 10^6 km^3, GEL ~8.3 m) [41]. The current polar caps are transient features, becoming unstable at increased obliquity [42]. **2) Alternate Volatile Reservoirs During Climate Change Evolution:** This survey supports the presence of several non-polar ice reservoirs that are currently not an active part of today's hydrological cycle but that were active in the Late Amazonian or earlier: 1) tropical mountain glaciers (TMG); 2) mid-latitude plateau and valley glaciers (MLG); 3) mid-high latitude regionally extensive ice mantles (LDM); 4) south circumpolar DAF. **3) Relationship of Climate Change Drivers and Alternate Volatile Reservoirs:** GCMs and related simulations support the interpretations that: 1) the current polar caps become unstable at obliquities >30° [42]; 2) LDMs form at obliquities between the current mean and ~35° [5]; 3) MLGs form at ~35° obliquity with appropriate dust opacity [43], 4) TMGs form at obliquities of ~45° [32]. Some uncertainty exists in the detailed transport mechanisms and timing [5, 32, 42]. **4) Sequestration: Evidence for Removal of Ice from the Active Climate System:** Abundant evidence (e.g., ring-mold craters (RMC) [20-21] and SHARAD data [22-23] in LDA/LVF and related deposits [38]; viscously relaxed craters [44] in TMGs; sublimation pits in pedestal craters [34]; RMCs, altimetry data, and surface textures in EECs [45]; and altimetry data and RMCs in CCF [14-15, 48] suggests that significant quantities of ice remain sequestered in association with ancient volatile reservoirs. These deposits have been sequestered by development of sublimation lags, sealing them off from significant participation in the current water cycle. This sequesterion represents a process of removal of water from the active system and a corresponding decrease in the total volume involved in the active water cycle with time. **5) Amazonian Climate History:** Analysis of Amazonian-aged deposits suggests that the climate was largely cold and hyperarid throughout the Amazonian, with variations in spin-axis/orbital parameters causing migration of ice from the poles to form equatorial and mid-latitude glaciers, and mid-high latitude regional blankets of snow and ice. Statistical studies suggest that typical Amazonian conditions did not include the presence of polar ice cap reservoirs [2]. **6) Transition to the Hesperian-Noachian Climate:** The DAF, interpreted as a volumetrically very significant sequestered ice deposit [40], represents a step-function in the evolution of the climate of Mars. Estimated current DAF volumes (~2.19 x 10^6 km^3; GEL ~15 m [40]) are close to the current combined polar cap volumes (GEL ~16) [41] and may be largely remnant water ice [46]. If the atmosphere was thicker during the Noachian and Hesperian eras than today, then conditions at the south pole may have been very different. For example, above a few hundred Pascals, surface temperature distribution would behave much more like on Earth, with high altitude regions significantly colder than lower plains because of adiabatic cooling of the atmosphere [47]. Within this context, it is likely that the high southern latitudes would have become a cold-trap where ice would tend to accumulate and form a large ice cap, because of both their latitude and altitude. The Hesperian-aged DAF suggests that conditions were different in this important transitional period, with the possibility of a thicker atmosphere producing the huge south-circumplolar DAF. These observations provide an important context for the assessment of the Noachian climate history of Mars. **7) History of Climate Change:** On the basis of the inventory of water-related deposits to date, the DAF appears to represent the sequestered record of a significantly different climate that characterized the early history of Mars. This was followed in the Amazonian by a hyperarid cold climate with a lower-volume water cycle dominated by mobilization and lateral migration of surface snow and ice in response to variations in spin-axis/orbital parameters; the active water inventory decreased with time due to progressive sequestration of snow and ice beneath sublimation lags [17-24].

References: 1) M. Carr, *Water on Mars*, 1996; 2) J. Laskar et al, *Icarus* 170, 343, 2004; 3) D. Marchant and J. Head, *Icarus* 192, 187, 2007; 4) M. Richardson and J. Wilson, *JGR* 107, 5031, 2002; 5) M. Mischna et al., *JGR* 108, 5062, 2003; 6) J. Head et al., *Micro 38* MS032, 2003; 7) J. Laskar et al, *Nature* 419, 375, 2004; 8) S. Milkovich and J. Head, *JGR* 110, 2349, 2004; 9) J. Head et al., *Nature* 426, 797, 2003; 10) R. Milliken et al., *JGR* 108, 2005, 2003; 11) J. Mustard et al., *Nature* 412, 4211, 2001; 12) J. Garvin et al. *MAPS* 41, 1659, 2006; 13) S. Squyres et al., *Mars*, U of AZ Press, 523, 1992; 14) M. Kreslavsky et al., *MAPS* 41, 1659, 2006; 15) J. Head et al., *Vernadsky-Brown Micro 46*, 2007; 16) B. Lucchitta, *JGR* 89, B409, 1984; 17) J. Head et al. *EPSL* 241, 663, 2006; 18) J. Head et al., *GRL* 33, L08S03, 2006; 19) J. Head and D. Marchant, *LPSC 37* #1126, 2006; 20) L. Ostrach and J. Head, *LPSC 38*, #1100, 2007; 21) A. Kress and J. Head, *GRL* 35, 35501, 2008; 22) J. Holt et al., *Science* 322, 1235, 2008; 23) J. Plaut et al., *GRL* 35, 36379, 2008; 24) J. Dickson et al. *Geology* 36, 411, 2008; 25) E. Hauber et al., *JGR* 113, EO2007, 2007; 26) J. Head and D. Marchant, *Geology* 31, 641, 2003; 27) D. Shean et al., *JGR* 110, 05001, 2005; 28) S. Kadish et al, *Icarus* 197, 84, 2008; 29) D. Shean et al, *JGR* 112, 2761, 2007; 30) S. Milkovich et al., *Icarus* 181, 388, 2006; 31) J. Head et al. *Nature* 44, 336, 2005; 32) F. Forget et al. *Science* 311, 368, 2006; 33) J. Head et al., *GRL* 31, L10701, 2004; 34) S. Kadish et al., *GRL* 35, L16104, 2008; 35) S. Kadish et al., *LPSC 39* 1766, 2008; 36) B. Black and S. Stewart, *JGR* 113, EO2015, 2008; 37) S. Meresse et al, *MAPS* 41, 1647, 2006); 38) G. Pederson and J. Head, *EPSC* A-00422, 2008; 39) K. Tanaka and E. Kolb, *Icarus* 154, 3, 2001; 40) J. Head and S. Pratt, *JGR* 106, 12275, 2001; 41) D. Smith et al., *JGR* 106, 23689, 2001; 42) B. Levrard et al, JGR 112, E06012, 2007; 43) J-B Madeleine et al, *LPSC 38* 1778, 2007; 44) J. Head and D. Marchant, *EMSEC-ESTEC*, 2007; 45) G. Pederson and J. Head, *LPSC 40*, 2008; 46) J. Plaut et al., *LPSC 38* 2144, 2007; 47) F. Forget et al., *AGU Fall Meeting*, P11A-0964, 2004; 48) J. Levy and J. Head, *EPSC2008* 00458, 2008.

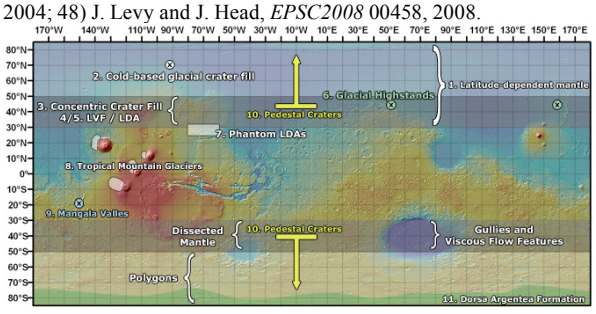

Part 2: Deciphering Late Amazonian Climate History-Assessing Obliquity Predictions: Introduction and Approach: Deciphering climate history has been one of the major goals of the scientific exploration of Mars because of the significance of climate as a proxy for understanding: 1) planetary volatile accretion, 2) outgassing history, 3) the distribution and stability of water and the nature and evolution of the water cycle, 4) the surface weathering environment, 5) the presence, stability, and abundance of liquid water, and 6) the implications for environments conducive to the origin and evolution of life [1]. Recent intensive exploration has contributed significantly to the understanding of current Mars weather, and lengthening observational baselines are beginning to reveal the basic elements of climate. This baseline knowledge is essential to the proper understanding of the longer-term history of climate. Assessing longer-term climate change and its history can be approached from a process-response standpoint through the identification of cause and effect [2] (Fig. 2). Among the most important causes of climate change (input parameters) are external forcing functions linked to spin-axis and orbital variations, elements whose nature and history have recently become much more well-understood in both the time and frequency domain [3]. The influence of these external forcing functions on the climate system (the internal response mechanism) are becoming more well known through increasingly more sophisticated atmospheric general circulation models [4-7], including the behavior of water. Finally, the consequences of the causes (the external forcing functions, spin-axis/orbital parameters, operating on the internal response mechanism, the climate system) produces an effect in the time and frequency domain (the geological record); increasing availability of global data is providing a more comprehensive view of over four billion years of geological history [8]. Specifically, increased knowledge of the structure of current polar deposits [9], the location of geological deposits that chronicle the distribution and history of non-polar ice [10], and the context in which to interpret ice deposits in extremely cold hyper-arid Mars-like conditions [11], have all contributed to an increased understanding of the climate history of Mars.

A robust prediction of the spin-axis/orbital parameter-based insolation input to the climate system has been developed for the last 20 Ma [3] and these predictions have been used to begin to decipher the history of the polar cap [12-14], the nature of recent ice ages [15], the timing of active layers at high latitudes [16], and the conditions under which liquid water might form gullies during this time [17]. Prior to the last 20 Ma, deterministic predictions are not currently possible because solutions based on the input parameters become chaotic; nevertheless exploring this parameter space, Laskar et al. produced 15 scenarios showing candidate obliquity histories over the last 250 Ma (Fig. 3), and predicted that mean obliquity would be ~38° [3]. Analysis of these 15 examples shows the huge range of options for Late Amazonian climate history. In contrast to the last 20 Ma, where input parameters to the climate system are well-known, there is no robust prediction for a specific input parameter history to use as a test in interpreting the geological record. Therefore, we have adopted a different approach and use the geological record of non-polar ice deposits [10] (the output of the external forcing function and climate system) and a general knowledge of the behavior of the GCM and climate system under different obliquity baselines, to evaluate the 15 candidate scenarios of the obliquity component of the external forcing function.

Analysis and Discussion: Using a general knowledge of the behavior of the GCM under different obliquity conditions, we chose four mean baselines to form a framework for evaluating the 15 candidate obliquity scenarios for the last 250 Ma: **Baseline 1 (~25°):** Current mean obliquity; robust water-ice polar caps, high-latitude ground ice [18], surface/near-surface ice unstable in equatorial and mid-latitude regions [19]. **Baseline 2 (~15°):** Very low mean obliquity; CO_2 atmosphere collapses, condenses at poles [20]; **Baseline 3 (~35°):** Intermediate mean obliquity; no polar cap [14], mid-latitude glaciation with appropriate dust opacity [21]. **Baseline 4 (~45°):** Moderate mean obliquity; equatorial reservoir dominates [22]; tropical mountain glaciers [23-28]. For the geological record, we use the summary of non-polar ice occurrences and chronology compiled in [10]. We now use these four mean baselines as a framework to evaluate the 15 candidate obliquity scenarios for the last 250 Ma. First, the 15 candidates can be classified into four different groups on the basis of total duration of time, and consistency of time, spent at different mean obliquities: **Group 1:** At or below 20° for periods of more than 100 Ma (Fig 3-1;10;11;13). **Group 2:** At or above 45° for periods of more than 100 Ma (Fig. 3-3;5;7;9;12;14). **Group 3:** Intermediate between these two mean values for the majority of the period (Fig. 3-2;4;6;8;15). Within these groups, clear variations are seen in: 1) the duration of time spent at a specific mean obliquity (compare 3-1 and 3-4); 2) the linearity or sinuosity of the mean obliquity path over 250 Ma (Fig. 3; compare 7, highly linear, with 4 and 15, highly sinuous); and 3) the episodicity of the amplitude of oscillations about the mean (Fig. 3-2; compare 50-125 Ma to 125-200 Ma BP).

We can now apply the geological observations, in terms of interpreted latitude and time [10], to assess the candidate obliquity scenarios. The Tharsis Montes tropical mountain glacier deposits (Arsia, Pavonis, Arcraeus) [24-26;29] have been dated to a period estimated to lie in the range between >50 Ma (superposed lava flows) and ~650 Ma (the deposit itself) [29], with Ascraeus ~25-380 Ma [25] and the nearby Olympus Mons glacial deposits in the 130-280 Ma range [30]. Recurring, smaller scale deposits were emplaced at Arsia in the last ~35-115 Ma (model age ~65 Ma) [26].

GCM simulations [21] predict the formation of mid-latitude glaciers in the northern mid-latitudes at ~35° obliquity with appropriate dust opacity; deposits interpreted to be mid-latitude glaciers [31-32] formed at ~ 200-300 Ma BP [33], and similar mid-latitude debris covered glaciers formed at about 75 Ma in the southern mid-latitudes [34]. The presence of these deposits in these time periods argues against all Group 1 (very low obliquity) candidate scenarios (1;10;11;13), all Group 2 (high obliquity) scenarios (3;5;7;9;12;14), and almost all Group 3 (intermediate obliquity) scenarios (2;4;6;15). The remaining candidate obliquity scenario that could plausibly be consistent with the age and obliquity constraints (Fig. 3-8) is characterized by 45° oblquity at the times of both the early and late TMGs, and obliquity at or close to 35° during mid-latitude glaciations.

Conclusions: Examination of the geological record of non-polar ice deposits can help significantly in distinguishing among candidate Late Amazonian obliquity histories. It is important to note that even the remaining candidate obliquity scenario (Fig. 3-8) is not necessarily the correct one as none of the solutions are deterministic; nonetheless, the ability to reject the vast majority of the candidate scenarios underlines the usefulness of the approach. Further, these results suggest that the actual obliquity history was not likely characterized by long-term (>150 Ma) periods at extreme values. Additional dating of these non-polar, ice-related deposits [10] can help populate the constraint space for the last 250 Ma, providing an increasingly more detailed and realistic Late Amazonian obliquity and climate history. Because spin-axis/orbital parameter prior to 20 Ma are not currently uniquely predictable [3], the geological record provides the basis to: 1) further test predictions, and 2) construct the actual obliquity history, one of the major input parameters necessary to characterize the Late Amazonian climate history. Similar approaches can be applied to earlier periods of Mars history.

Implications for History of the Hydrological Cycle: The style of these preserved ice-related deposits and correlations outline a long history during which a horizontally stratified hydrologic cycle has apparently prevailed. The latest Noachian-earliest Hesperian appears to be the most likely time in which a vertically integrated hydrologic cycle might have characterized Mars.

References: 1) M. Carr, *Water on Mars*, 1996; 2) J. Imbrie, *Icarus* 50, 408, 1982; 3) J. Laskar et al, *Icarus* 170, 343, 2004; 4) F. Forget et al., *JGR* 104, 24155, 1999; 5) M. Richardson and J. Wilson, *JGR* 107, 5031, 2002; 6) M. Mischna et al., *JGR* 108, 5062, 2003; 7) R. Haberle et al., *JGR* 106, 23317, 2003; 8) M. Carr, *The Surface of Mars*, Cambridge, 2006; 9) R. Phillips et al., *Science* 320, 1182, 2008; 10) J. Head and D. Marchant, *LPSC 39* 1295, 2008 and this volume; 11) D. Marchant and J. Head, *Icarus* 192, 187, 2007; 12) J. Laskar et al, *Nature* 419, 375, 2004;13) S. Milkovich and J. Head, *JGR* 110, 2349, 2004; 14) B. Levrard et al, JGR 112, E06012, 2007; 15) J. Head et al., *Nature* 426, 797, 2003; 16) M. Kreslavsky et al., *MAPS* 41, 1659, 2006; 17) F. Costard et al. *Science* 295, 110, 2002; 18) W. Boynton et al., Science 296, 8, 2002; 19) M. Mellon and B. Jakosky, *JGR* 100, 11781, 1995; 20) M. Kreslavsky and J. Head, *GRL* 32, L12202, 2005; 21) J-B Madeleine et al, *LPSC 38* 1778, 2008; 22) F. Forget et al. *Science* 311, 368, 2006; 23) J. Head and D. Marchant, *Geology* 31, 641, 2003; 24) D. Shean et al., *JGR* 110, 05001, 2005; 25) S. Kadish et al, *Icarus* 197, 84, 2008; 26) D. Shean et al, *JGR* 112, 2761, 2007; 27) S. Milkovich et al., *Icarus* 181, 388, 2006; 28) J. Fastook et al., *Icarus* 198, 305, 2008; 29) D. Shean et al. *LPSC 37* 2092, 2006; 30) G. Neukum et al., *Nature* 432,971, 2004; 31) J. Head et al. *EPSL* 241, 663, 2006; 32) J. Head et al., *GRL* 33, L08S03, 2006; 33) N. Mangold, *JGR* 108, 8021, 2003; 34) J. Head et al. *Nature* 44, 336, 2005.

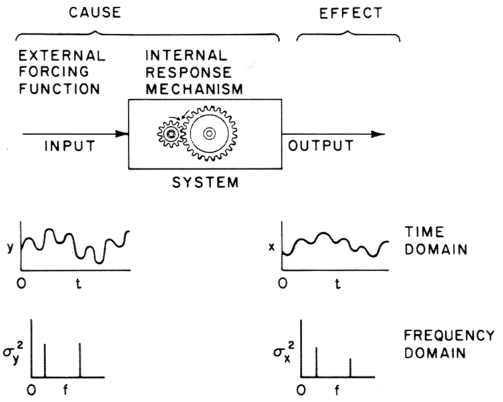

Fig. 2. Process-response framework for analysis of the climate system on Mars [2].

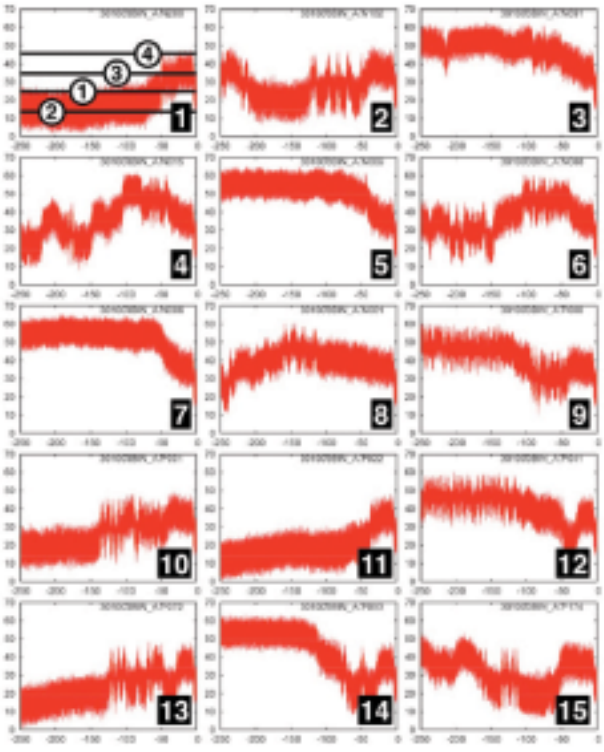

Fig. 3. Examples of possible evolution of Mars' obliquity over the past 250 Myr [3]. In the text, candidate examples are numbered from 1-15, starting in the upper left (1) and working across rows (2-3) in each of the five successive rows.

Acknowledgements: Thanks are extended to D. Marchant, F. Forget, J. Laskar, J.-B. Madeleine, J. Fastook, J. Levy, C. Fassett, G. Morgan, L. Kerber, J. Dickson, D. Shean, S. Kadish, S. Schon, D. Baker, A. Kress, L. Ostrach and S. Millkovich for contributions to this work.